Surface Chemistry

International Edition: DOI: 10.1002/anie.201804110
German Edition: DOI: 10.1002/ange.201804110

On-Surface Bottom-Up Synthesis of Azine Derivatives Displaying Strong Acceptor Behavior

*Nerea Ruiz del Árbol, Irene Palacio, Gonzalo Otero-Irurueta, José I. Martínez, Pedro L. de Andrés, Oleksander Stetsovych, María Moro-Lagares, Pingo Mutombo, Martin Svec, Pavel Jelínek, Albano Cossaro, Luca Floreano, Gary J. Ellis, María F. López, and José A. Martín-Gago**

Abstract: *On-surface synthesis is an emerging approach to obtain, in a single step, precisely defined chemical species that cannot be obtained by other synthetic routes. The control of the electronic structure of organic/metal interfaces is crucial for defining the performance of many optoelectronic devices. A facile on-surface chemistry route has now been used to synthesize the strong electron-acceptor organic molecule quinoneazine directly on a Cu(110) surface, via thermally activated covalent coupling of para-aminophenol precursors. The mechanism is described using a combination of in situ surface characterization techniques and theoretical methods. Owing to a strong surface-molecule interaction, the quinoneazine molecule accommodates 1.2 electrons at its carbonyl ends, inducing an intramolecular charge redistribution and leading to partial conjugation of the rings, conferring azo-character at the nitrogen sites.*

Organic heterostructures based on electron acceptor–donor organic molecules on surfaces have become strategic materials owing to their huge technological impact in fields such as organic light-emitting diodes (OLEDs), organic field effect transistors (OFETs), or solar cell devices, amongst others. In electronic devices, organic layers are placed on metallic surfaces for electrical contact, and the structure of the metal–organic interface enormously affects the performance.[1] In particular, some molecules promote charge transfer at the interface with metal electrodes owing to their donor (acceptor) nature, which may induce energy level realignment that can be exploited to tune the transport properties of the system.[1–5] Despite the potential impact of this approach, only a few molecules have been shown to efficiently donate (or accept) significant charge, this quality being related to the presence of donor (acceptor) moieties in their structures.[6] A typical example is tetracyano-*p*-quinodimethane (TCNQ), a strong acceptor molecule that when deposited on Cu(100) accommodates around 1.6 electrons whereby almost one electron aromatizes the central hexagonal ring and the remaining fraction of the charge is accommodated in one of the peripheral nitrogen atoms of the cyano groups.[3]

On the other hand, on-surface synthesis can generate unique molecules or extended molecular architectures that have been rationally formed via alternative synthetic routes to those available through solution-based chemistry.[7,8] These surface-stabilized species can lead to compounds that are difficult or impossible to obtain via conventional synthetic procedures.[9–12]

Herein, we combine both of the aforementioned features. We show that the on-surface coupling reaction of two simple and inexpensive *para*-aminophenol (*p*-Ap) molecules can be employed to form a quinonoid-like derivative, quinoneazine (QAz). This molecule has been theoretically proposed for organic electrodes owing to their extreme redox voltages, and it can also be employed as an intermediate in the preparation of several chemically and biologically active compounds.[13,14] We show that, similar to the case of TCNQ molecules, the on-surface synthesized QAz molecule can accept about 1.2 electrons from the Cu surface through a strong interaction with the surface atoms. We observe that the role of the surface is two-fold. Firstly, it catalyzes the synthesis of QAz, a non-aromatic compound difficult to obtain by conventional synthesis routes.[15] Secondly, it stabilizes the molecular structure by donating to the QAz more than one electron to form a resonant structure, see Scheme 1, as we will discuss below.

We used a combination of several surface-science experimental techniques, including synchrotron radiation-based X-

[*] N. Ruiz del Árbol, I. Palacio, J. I. Martínez, P. L. de Andrés, M. F. López, Prof. J. A. Martín-Gago
ESISNA Group, Materials Science Factory. Institute of Materials Science of Madrid (ICMM-CSIC)
Sor Juana Inés de la Cruz 3, 28049 Madrid (Spain)
E-mail: gago@icmm.csic.es

G. Otero-Irurueta
Centre for Mechanical Technology and Automation (TEMA)
University of Aveiro
3810-193 Aveiro (Portugal)

O. Stetsovych, M. Moro-Lagares, P. Mutombo, M. Svec, P. Jelínek
Institute of Physics, Academy of Sciences of the Czech Republic
Cukrovarnicka 10, 1862 53 Prague (Czech Republic)

A. Cossaro, L. Floreano
Laboratorio TASC, CNR-IOM
Basovizza SS-14, Km 163.5, 34149 Trieste (Italy)

G. J. Ellis
Polymer Physics Group
Institute of Polymer Science and Technology (ICTP-CSIC)
Juan de la Cierva 3, 28006 Madrid (Spain)

Supporting information and the ORCID identification number(s) for the author(s) of this article can be found under: https://doi.org/10.1002/anie.201804110.

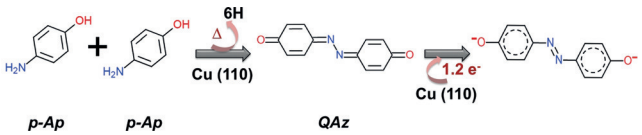

Scheme 1. Azine-coupling of *p*-aminophenol precursors (*p*-Ap) to form quinoneazine (QAz) via thermally induced reaction of two *p*-aminophenol molecules on Cu(110) surfaces.

ray photoemission spectroscopy (XPS) and near-edge X-ray absorption fine structure (NEXAFS), scanning tunneling microscopy (STM), and non-contact atomic force microscopy (nc-AFM), supported by first-principles theoretical calculations (details are provided in the Supporting Information). This large battery of tools allows us to obtain a full and consistent picture of this unusual on-surface chemical reaction and the strong charge redistribution process occurring at the organic–metal interface.

The starting point of our method is the evaporation in ultra-high vacuum (UHV) of *p*-Ap molecules on an atomically clean Cu(110) surface. Depending on the surface temperature during evaporation, we observe two distinct cases: the adsorption at room temperature leads to individual *p*-Ap molecules adsorbed on the surface (RT phase, Figure 1 a), and the evaporation onto the surface at 520 K (HT phase, Figure 1 b), where molecular structures exhibiting long-range ordered and a uniform, well-defined surface morphology is found. The HT phase can also be obtained by direct annealing of the RT phase at 520 K, displaying equivalent results.

The size and shape of the circular features dispersed across the surface observed in the STM image of Figure 1 a correspond to single *p*-Ap molecules,[16] and the nc-AFM image (in the inset) clearly shows the hexagonal carbon rings confirming the presence of single isolated molecules. They form locally a 4×4 superperiodicity. In contrast, in the STM image in Figure 1 b the surface molecular species observed are larger and elliptical in shape and of uniform size, with a bright feature in the center. Further, they are well-organized into precisely aligned linear rows oriented at an angle of 20° with respect to the [001] surface direction (Supporting Information, Figure S3). The LEED pattern (see inset) indicates that the molecular arrangement is commensurate with the substrate suggesting that the Cu(110) crystal termination plays a fundamental role in the process of the formation of the HT phase.

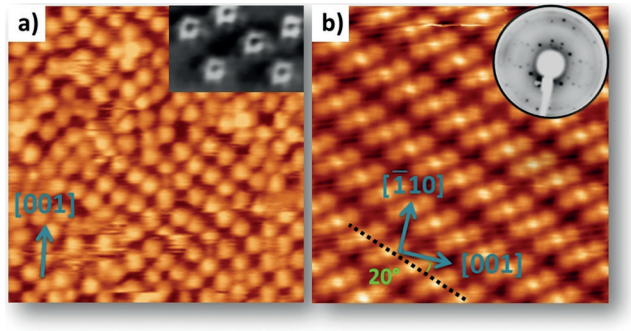

Figure 1. STM images (7.7×7.7 nm^2). a) Constant-current image recorded at RT with $V_{bias}=+1$ V and $I_{tunnel}=141$ pA, where the single bright spots are individual *p*-Ap molecules. The inset shows a nc-AFM with a functionalized tip of some adsorbed *p*-Ap molecules, and b) constant height image recorded at 5 K after deposition of *p*-AP at 520 K, where larger molecular species with clearly defined size, and orientation are seen. (1 mV,5 pA). Inset: a LEED pattern exhibiting a long-range order with a [(5, 1), (−1, 2)] symmetry with the substrate (electron energy = 33 eV).

The chemical structure of the RT and HT phases can be unequivocally followed in situ by high-resolution XPS and NEXAFS (see the Supporting Information). Figure 2 shows the XPS core-level peaks of the elements of the *p*-Ap precursors, N 1s, O 1s, and C 1s, and their evolution with coverage and temperature. The C 1s spectrum displays no significant core-level shift with respect to the multilayer and in all cases the components associated with the four sp^2 carbons cannot be individually resolved, in agreement with a recent study on hydroxycyanobenzene,[17] and indicating

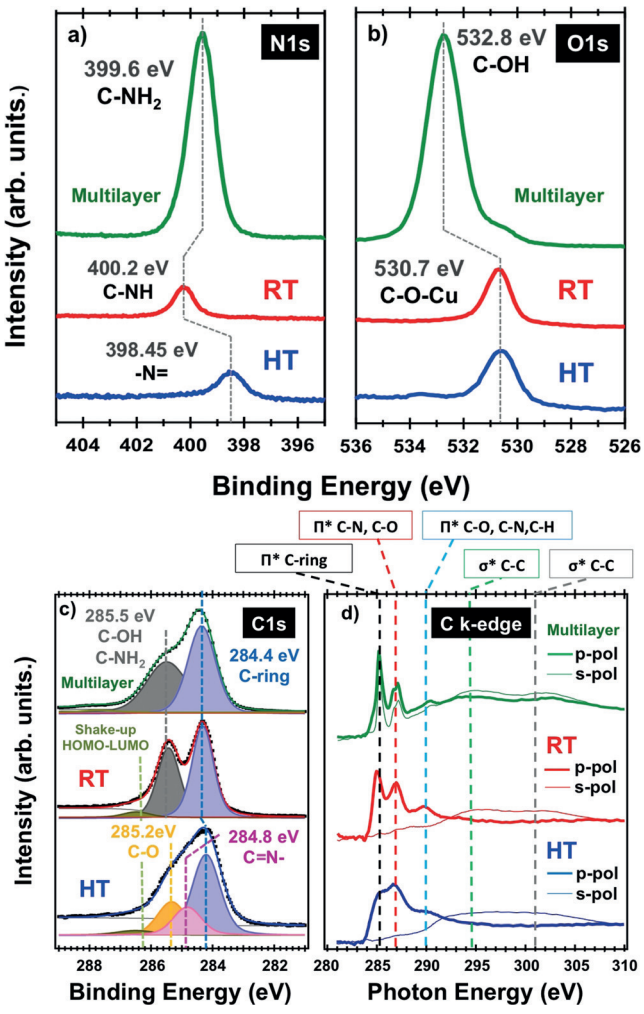

Figure 2. a),b),c) N 1s, O 1s, and C 1s XPS spectra for a physisorbed multilayer (green curve) self-assembled monolayer at RT (red curve, RT phase) and at 520 K (blue curve, HT phase). The photon energies are, 500, 650, and 400 eV, respectively. d) NEXAFS spectra for C k-edge for the same phases recorded at s-polarization (electric field vector parallel to the surface) and p-polarization (electric field vector perpendicular to the surface).

that the atoms of the carbon ring do not participate in the surface chemical reaction. On the contrary, the N 1s and O 1s peaks in the (sub)monolayer RT phase display large core-level shifts (in opposite directions), indicating that the *p*-Ap precursor adsorbs in its oxidized form (red spectra in Figure 2). Both hydroxy and primary amine moieties of the *p*-Ap molecules deprotonate to generate phenoxy and secondary amine groups.[18,19] However, when *p*-Ap is dosed at high temperature (520 K, blue curve labeled HT in Figure 2), a significant shift to lower binding energy of the N 1s peak with respect to the RT layer indicates the full oxidation of the amine terminations into their iminic form.[20,21]

The overall intensities of the C 1s, N 1s, and O 1s peaks show no significant change upon heating, indicating that the process does not affect the stoichiometry of the molecular layer. However, an overall small shift of the C 1s spectrum towards lower binding energy is observed, indicating that carbon atoms have accepted charge.[21,22] We may conclude that a dimerization reaction between two adjacent *p*-Ap molecules takes place via surface-mediated thermally induced covalent coupling of the NH species, to generate an azine bond leading to the QAz molecule.

To obtain further insights into the structure of the HT phase and the role of the surface, we used NEXAFS spectroscopy. By varying the surface orientation with respect to the linear polarization of the incident light in NEXAFS, the spectral response corresponding to the π*-symmetry components shows dichroic anisotropy (Figure 2 d).[23] The curve that corresponds to the multilayer *p*-Ap presents no important variations with polarization. However, both RT and HT phases show a strong enhancement of the π* part of the spectra in p-polarization and quenching in s-polarization. This dichroic behavior indicates that the carbon ring is oriented parallel to the metal surface, with an average tilt of 5°, in good agreement with the STM images and calculations (Figure 3 a). Moreover, the change of shape of the NEXAFS spectra (overall quenching and shift to lower energy of the first resonance) indicates a net charge transfer from the surface to the lowest molecular orbital (LUMO) localized on the carbon ring.

The nc-AFM images of the HT phase (Figure 3 b) show intramolecular features with two bright protrusions that can be assigned to two equivalent ring structures linked together as a covalent dimer. Simulations of the nc-AFM images using a probe particle model[24] are in close agreement with the experimental data. Moreover, although an apparent chain-like structure is often seen in STM images, simulations rule out any polymerization of the precursors, and the chain appearance of the images is related to a modification of the electronic properties of the last Cu layer owing to the strong interaction with the QAz molecule (Supporting Information, Figure S10).

DFT calculations show that QAz prefers to be stacked along a direction forming a 20° angle with respect to the [001] crystallographic axis of the Cu substrate, in agreement with the LEED measurements. The optimized ground-state structure shows both terminating oxygen atoms at nearly-on-top positions of the Cu atoms, at an average perpendicular

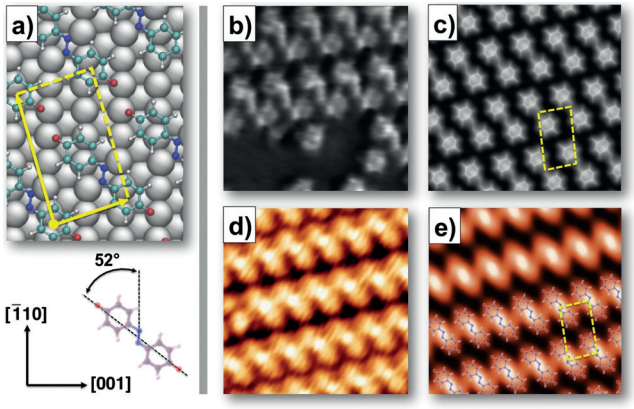

Figure 3. a) DFT optimized geometry of QAz molecules on Cu(110), represented for only the first layer of the substrate. The main symmetry axis of QAz (from one oxygen to the other presented in the structure) are at 52° with respect to the [1̄10] direction of the substrate. The oxygen atoms are bound to the Cu (110) at bridge positions. The substrate directions are indicated in the Scheme and the unit cell indicated in yellow. b) Frequency-shift (force) image acquired by nc-AFM/STM with a functionalized probe at 5 K. c) AFM image simulation of optimized QAz/Cu(110) configuration using the probe particle AFM model. d) Experimental STM image of QAz formed in the HT phase recorded at RT. $V_{bias} = +1350$ mV and $I_{tunnel} = 31$ pA. e) Computed Keldish–Green STM image under the same experimental conditions as (d).

distance from the substrate of around 2.0 Å. This configuration steers both N atoms to a symmetrical bridge site. Both carbon rings are essentially symmetrical with a slight axial tilt of 4.5° along the stacking direction, in good agreement with the experimental NEXAFS value of about 5°. A N–N bond length of 1.31 Å was obtained that is slightly longer than values reported for gas-phase azobenzene,[25] or gas-phase dimetacyano-azobenzene (DMC), which range from 1.27 to 1.29 Å.[20,26] Interestingly, the QAz molecule does not structurally deform on the surface, whereas in the case of TCNQ, porphyrins, or other donor–acceptor blends, the active moieties need to modify their structure to strongly bond to the surface.[2–4]

STM provides further indirect proof for the azine linkage. Firstly, no configurational isomers (*cis–trans* forms) typical of azo-groups are found, not even at the island borders or steps, where such molecular structures might be more easily accommodated. Secondly, the STM images show a bright protrusion in the center of the dimer, that is, at the N–N position, which can be qualitatively attributed to a charge density increase due to the formation of the covalent bond in the QAz molecule. In an azo-coupled molecule, such as azobenzene, two independent lobes are observed at the rings with a depression in the center of the molecule.[25]

The net electronic charge transferred from the substrate to the QAz molecule was calculated by integration of the computed charge density difference (Figure 4 a), resulting in a value of 1.21 e^- per molecule. The large amount of electronic charge gained by the QAz molecule, resulting from the very different electronegativities of the Cu surface and the dimer (−2.07 eV in the gas phase), is redistributed within the molecule according to Figure 4 b. This shows

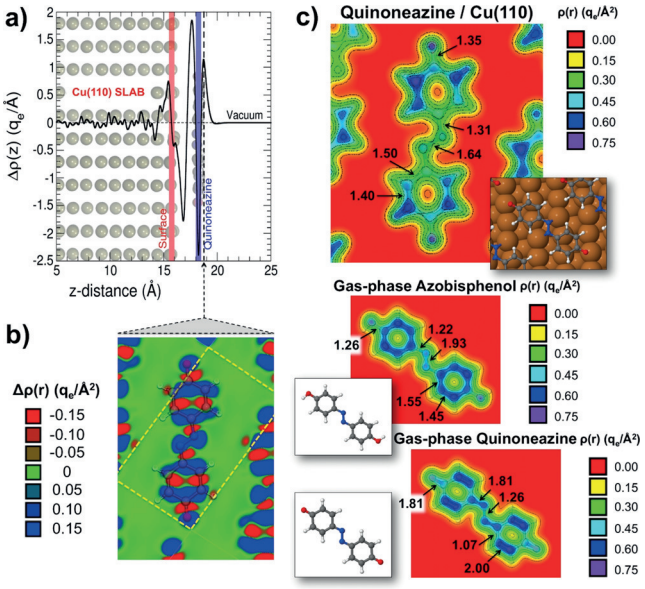

Figure 4. a) Computed plane-averaged charge density difference, $\Delta\rho(r)$ in $q_e Å^{-1}$ units, for the optimized QAz/Cu(110) configuration along the *z*-direction. Vertical red and blue lines indicate the average *z*-positions for the topmost Cu layer and the flat-lying molecule. b) Surface charge-density difference w.r.t. the gas-phase moiety, $\Delta\rho(r)$ in $q_e Å^{-2}$ units, color map for the optimized QAz/Cu(110) configuration in the *xy*-plane at $z = 0.6$ Å above the average *z*-position of the molecule (see vertical dashed black line in (a)). c) Surface charge density, $\rho(r)$ in $q_e Å^{-2}$ units, color map in the xy-plane at $z = 1$ Å above the average *z*-position of the molecule for: (top) the optimized QAz/Cu(110) configuration, (middle) the optimized gas-phase azobisphenol molecule, and (bottom) the optimized quinoneazine molecule. For the three cases, the computed Pauling bond orders for the most representative bonds are included.

a computed 2D color map of the surface charge density difference, defined as $\Delta\rho(r) = \rho_{mol/Cu}(r) - [\rho_{mol}(r) + \rho_{Cu}(r)]$, where $\rho_{mol/Cu}(r)$ is the spatial charge density of the QAz/Cu(110) system, and $\rho_{mol}(r)$ and $\rho_{Cu}(r)$ the spatial charge densities of the non-interacting QAz, and the Cu(110) with the geometry they adopt at the interface. The red and blue regions denote a loss or gain, respectively in the net charge after the formation of the interface. These regions that correspond to the maximum charge displacement are spatially localized, mostly in three critical zones: 1) charge accumulation at the two terminating C–O moieties; 2) charge depletion at the two C–N bonds and accumulation between the N atoms; and 3) redistribution within the ring to the four lateral C=C bonds.

Figure 4a,b illustrates the significant charge reorganization at the interface and strong bonding with the surface, with a strong depletion of electronic density located just above the topmost Cu layer (see also the Supporting Information, Figure S10). Figure 4c shows surface charge density color maps of the QAz and ABP molecules in the gas phase, and for the optimized QAz molecule on a Cu(110) surface, where a close similarity to the aforementioned azo-compound can be observed, mainly at N and O sites as well lateral sites in the C rings. Pauling bond-order analysis is a powerful strategy to rationalize aromaticity on organic molecules.[27] To numerically quantify the charge rearrangement within, each bond we have determined the bond-order for the three cases of Figure 4c revealing that O–C, C–N and N–N bonds are single, single, and double, respectively, for gas-phase ABP and double, double, single, for QAz. Aromaticity in the C rings for gas-phase ABP is also observed, but not for the gas-phase QAz. Interestingly, the same Pauling analysis carried out on the molecules at the QAz/Cu(110) interface shows a flip in the bond orders of the molecular bonds with respect to QAz in the gas phase, becoming effectively more similar to those found for gas-phase ABP (Supporting Information, Table S1). Furthermore, the interfacial interaction and significant charge redistribution in the system generates a strong adsorbate-induced dipole at the surface with the negative end pointing towards vacuum, hence increasing the work function.

In conclusion, we have shown that the on surface-synthetized azine-coupled QAz molecule extracts about 1.2 extra electrons from the metal surface inducing a strong intramolecular charge reorganization, which is accommodated throughout the molecule resulting in a partial recovery of the aromatic character of the rings and inducing an azo-like character at the N–N linkage, as shown by bond-order analysis. The choice of the precursors determines the charge transfer direction at the metal–organic interface, while the metal surface plays a crucial role in mediating both the synthesis and the charge transfer. Strong interaction between the surface and the molecule beyond self-assembly is necessary for an efficient charge transfer. Our work suggests a promising and novel route to the synthesis of hybrid organometallic electrodes with predictable electronic properties, and opens the door for the use of on-surface synthesis protocols to fabricate á la carte donor or acceptor interfaces on organic heterostructures.

Acknowledgements

Graphene Flagship Core2-Graphene-based disruptive technologies EU Horizon 2020 (785219), ERC-synergy program (ERC-2013-SYG-610256 Nanocosmos), CTI-CSIC and Spanish MINECO (grants MAT2017-85089-C2-1-R, MAT2014-54231-C4-1-P, and MAT2014-54231-C4-4-P) are acknowledged. We are grateful to the Czech GACR funding (grant 17-24210Y) and LM2015087, Czech Academy of Sciences through the Praemium Academiae award and FCT program (IF/01054/2015).

Conflict of interest

The authors declare no conflict of interest.

Keywords: ab initio calculations · charge transfer · photoelectron spectroscopy · scanning probe microscopy · surface chemistry

How to cite: *Angew. Chem. Int. Ed.* **2018**, *57*, 8582–8586
Angew. Chem. **2018**, *130*, 8718–8722

[1] R. Otero, A. L. Vázquez de Parga, J. M. Gallego, *Surf. Sci. Rep.* **2017**, *72*, 105 – 145.
[2] T. Meier, R. Pawlak, S. Kawai, Y. Geng, X. Liu, S. Decurtins, P. Hapala, A. Baratoff, S. X. Liu, P. Jelínek, et al., *ACS Nano* **2017**, *11*, 8413 – 8420.
[3] T. C. Tseng, C. Urban, Y. Wang, R. Otero, S. L. Tait, M. Alcamí, D. Écija, M. Trelka, J. M. Gallego, N. Lin, et al., *Nat. Chem.* **2010**, *2*, 374 – 379.
[4] G. Zamborlini, D. Lüftner, Z. Feng, B. Kollmann, P. Puschnig, C. Dri, M. Panighel, G. Di Santo, A. Goldoni, G. Comelli, et al., *Nat. Commun.* **2017**, *8*, 1 – 7.
[5] M. Hollerer, D. Lüftner, P. Hurdax, T. Ules, S. Soubatch, F. S. Tautz, G. Koller, P. Puschnig, M. Sterrer, M. G. Ramsey, *ACS Nano* **2017**, *11*, 6252 – 6260.
[6] E. Goiri, P. Borghetti, A. El-Sayed, J. E. Ortega, D. G. De Oteyza, *Adv. Mater.* **2016**, *28*, 1340 – 1368.
[7] J. Méndez, M. F. López, J. A. Martín-Gago, *Chem. Soc. Rev.* **2011**, *40*, 4578.
[8] R. Lindner, A. Kühnle, *ChemPhysChem* **2015**, *16*, 1582 – 1592.
[9] G. Otero, G. Biddau, C. Sánchez-Sánchez, R. Caillard, M. F. López, C. Rogero, F. J. Palomares, N. Cabello, M. A. Basanta, J. Ortega, et al., *Nature* **2008**, *454*, 865 – 868.
[10] J. R. Sanchez-Valencia, T. Dienel, O. Gröning, I. Shorubalko, A. Mueller, M. Jansen, K. Amsharov, P. Ruffieux, R. Fasel, *Nature* **2014**, *512*, 61 – 64.
[11] O. Stetsovych, M. Švec, J. Vacek, J. V. Chocholoušová, A. Jančařík, J. Rybáček, K. Kosmider, I. G. Stará, P. Jelínek, I. Starý, *Nat. Chem.* **2017**, *9*, 213 – 218.
[12] D. Toffoli, M. Stredansky, Z. Feng, G. Balducci, S. Furlan, M. Stener, H. Ustunel, D. Cvetko, G. Kladnik, A. Morgante, et al., *Chem. Sci.* **2017**, *8*, 3789 – 3798.
[13] J. Safari, S. Gandomi-Ravandi, *RSC Adv.* **2014**, *4*, 46224 – 46249.
[14] D. Tomerini, C. Gatti, C. Frayret, *Phys. Chem. Chem. Phys.* **2015**, *17*, 8604 – 8608.
[15] R. Willstätter, M. Benz, *Ber. Dtsch. Chem. Ges.* **1907**, *40*, 1578 – 1584.
[16] G. Otero-Irurueta, J. I. Martínez, R. A. Bueno, F. J. Palomares, H. J. Salavagione, M. K. Singh, J. Méndez, G. J. Ellis, M. F. López, J. A. Martín-Gago, *Surf. Sci.* **2016**, *646*, 5 – 12.
[17] G. Olivieri, A. Cossaro, E. Capria, L. Benevoli, M. Coreno, M. De Simone, K. C. Prince, G. Kladnik, D. Cvetko, B. Fraboni, et al., *J. Phys. Chem. C* **2015**, *119*, 121 – 129.
[18] N. V. Richardson, P. Hofmann, *Vacuum* **1983**, *33*, 793 – 796.
[19] R. V. Plank, N. J. DiNardo, J. M. Vohs, *Surf. Sci.* **1995**, *340*, L971 – L977.
[20] M. Piantek, J. Miguel, A. Krüger, C. Navío, M. Bernien, D. K. Ball, K. Hermann, W. Kuch, *J. Phys. Chem. C* **2009**, *113*, 20307 – 20315.
[21] K. Diller, F. Klappenberger, M. Marschall, K. Hermann, A. Nefedov, C. Wöll, J. V. Barth, *J. Chem. Phys.* **2012**, *136*, 014705.
[22] F. Bebensee, K. Svane, C. Bombis, F. Masini, S. Klyatskaya, F. Besenbacher, M. Ruben, B. Hammer, T. Linderoth, *Chem. Commun.* **2013**, *49*, 9308.
[23] J. Stöhr, D. A. Outka, *Phys. Rev. B* **1987**, *36*, 7891 – 7905.
[24] P. Hapala, G. Kichin, C. Wagner, F. S. Tautz, R. Temirov, P. Jelínek, *Phys. Rev. B* **2014**, *90*, 1 – 9.
[25] C. R. Crecca, A. E. Roitberg, *J. Phys. Chem. A* **2006**, *110*, 8188 – 8203.
[26] N. Henningsen, R. Rurali, K. J. Franke, I. Fernández-Torrente, J. I. Pascual, *Appl. Phys. A* **2008**, *93*, 241 – 246.
[27] L. Gross, F. Mohn, N. Moll, B. Schuler, A. Criado, E. Guitian, D. Pena, A. Gourdon, G. Meyer, *Science* **2012**, *337*, 1326 – 1329.

Manuscript received: April 6, 2018
Version of record online: June 21, 2018

